Wafer-level fabrication of low power consumption integrated alcohol microsensor

Hairong Wang[1,2] ✉, *Mengya Wang*[1,2], *Weitao Lei*[1,2], *Xiaowei Chen*[1,2], *Hao Huang*[1,2], *Jiuhong Wang*[1,2]

[1]*School of Mechanical Engineering, Xi'an Jiaotong University, Xi'an 710049, People's Republic of China*
[2]*State Key Laboratory for Manufacturing Systems Engineering, Xi'an 710054, People's Republic of China*
✉ *E-mail: whairong@mail.xjtu.edu.cn*

Published in Micro & Nano Letters; Received on 18th May 2018; Revised on 10th August 2018; Accepted on 10th September 2018

An integrated alcohol microgas sensor was designed and fabricated based on TiO_2/SnO_2 nanocomposites acting as a sensing layer and microheater providing working temperature. The stacked TiO_2/SnO_2 nanocomposites were prepared by magnetron sputtering. A unique suspended membrane consisting of $Si_3N_4/SiO_2/Si_3N_4/SiO_2$ four layers was prepared by different methods, respectively, and applied in microheater to support the electrodes and sensing layer for reducing power consumption. The fabrication process tackled the difficulty that the sensing layer preparation is incompatible with microelectromechanical systems micromachining technology and realised the mass production of the wafer-level sensor chips with good consistency. The microalcohol sensors showed excellent response characteristics for alcohol (50–600 ppm) detection at low power consumption (39 mW).

1. Introduction: Gas sensors are of vital importance in modern society, which are employed to ensure that levels of various gases are within an acceptable range, such as H_2, NH_3, and volatile organic chemicals [1]. Among them, alcohol sensors are needed in many fields, such as industry, environment, human monitoring and so on [2]. The sensors based on metal–oxide semiconductor (MOS) materials have attracted lots of attention among the much types of gas sensors because of fast response, low detection limit, small size, measurement simplicity, and easy of fabrication [3–5]. However, a conventional MOS sensor usually operates at 300°C or higher, requiring hundreds of milliwatts of power consumption which is hardly satisfied on the battery-powered occasion [6].

To realise the purpose of low power consumption, integration of MOS nanostructured materials with microheater based on microelectromechanical systems (MEMS) technologies is an effective way and has been paid increasing attentions by researchers [7–12]. However, there are considerable challenges to realise the preparation of MOS nanostructured materials with excellent response characteristics and low power consumption for a gas sensor at the same time. This is because that process of preparing the nanostructured sensing materials is usually not compatible with micromachining technology of fabricating the microheater. We have previously reported a hierarchical nanostructured TiO_2 material grown onto the microheater through the vapour oxidation process, which has the potential risk to damage the fabricated microheating electrodes [12, 13]. Ink-jet printing is also a common method by dripping the nanoparticle paste onto the microheater to prepare a gas sensor with low power consumption [14]. In addition, the sol–gel methods are often used to prepare the sensing material [15, 16]. However, one may find that the above methods are not suitable for mass production on account of poor consistency, low yield, and high cost.

Magnetron sputtering is a typical thin film deposition process. It can precisely control chemical composition, the thickness of sensing materials by controlling the parameters such as sputtering power, sputtering time and so on [17, 18]. Magnetron sputtering can be considered to be compatible with MEMS technologies. When it is applied to deposit the gas sensing materials, the process can be arranged as an insertion process of fabricating the micro sensor chip, making it possible to fabricate the gas sensor chips on a wafer level. However, as the gas sensing material, the film deposited by magnetron sputtering is usually dense with the small specific area, resulting in lower sensitivity for the target gas. To improve the gas response characteristics, researchers turned to other techniques, e.g. doping the precious metal during film deposition or alternately depositing two materials to form a multiple layers composite [19–22].

In this Letter, we presented the design and fabrication process of an integrated microgas sensor based on stacked TiO_2/SnO_2 nanocomposites and microheater, which has low power consumption and excellent response characteristics for alcohol detection. The stacked TiO_2/SnO_2 nanocomposites prepared by magnetron sputtering have high sensitivity because of the formation of TiO_2/SnO_2 n–n heterojunction and higher specific surface area compared with single TiO_2. The microheater adopted a unique suspended membrane with a multilayer structure to support heating electrodes, sensing electrodes and sensing materials, aiming at reducing the power consumption and improving the mechanical strength. The integrated microgas sensors were designed and fabricated under the wafer level. The sensors' responses to alcohol were tested and the results indicated that the wafer-level gas sensors had characteristics of mass production, high yield, and good consistency.

2. Design and fabrication: The schematic design of the integrated microsensor chip is illustrated in Fig. 1. N-doped silicon wafer (4 inches) is chosen as the substrate. The primary design goal is to maximise the thermal efficiency to minimise the power consumption. Therefore, a unique suspended membrane structure is adopted, in which the silicon substrate under the heating area is totally released because of its high thermal conductivity and a 1.3 μm thick suspended membrane is remained. The suspended membrane is a multilayer structure consisting of 150 nm thick Si_3N_4 and 500 nm thick SiO_2. Different kinds of the thin films exhibit different stress state, which is caused by the intrinsic stress, unmatched thermal expansion and so on. The four layers of Si_3N_4, SiO_2, Si_3N_4 and SiO_2 thin films are fabricated by different methods to obtain stress compensation between different thin films. Compared with the common two films of Si_3N_4 and SiO_2, the suspended membrane with a multilayer structure should have less whole stress and higher mechanical strength [5, 12]. It is expected to have good thermal insulation and mechanical properties to support the electrodes and sensing materials above it. The backside of the silicon substrate has an insulating layer consisting of Si_3N_4 and SiO_2 two films, which are used as the masking layer for the wet etching. The sensing layer is a kind of nanocomposite, which has six layers of stacked SnO_2 and TiO_2

© The Institution of Engineering and Technology 2018

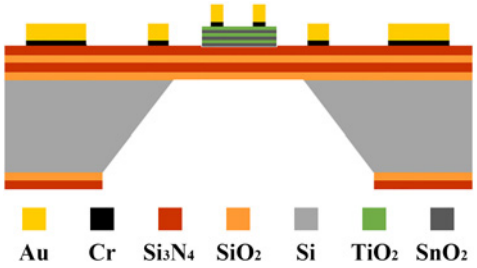

Fig. 1 *Schematic diagram of the integrated microalcohol sensor chip*

thin films in turn. The nanocomposite is located in the centre of the chip, which is the sensing material for perceiving the target gas. It can convert concentration change of the target gas into resistance change of the sensor chip at a proper temperature and the signal can be read out by the sensing electrodes.

The top view of the microsensor chip, with the size of $2000 \times 2000\ \mu m^2$, is illustrated in Fig. 2. To simplify the fabrication process, i.e. increase the yield and avoid the parasitic electric fields coming from embedding structure, heating electrodes and sensing electrodes are placed in the same layer with the same materials. The temperature sensors designed on the periphery of heating electrodes can monitor the temperature change of central area through their different resistance under different temperature. The electrodes materials are 250 nm thick Au film with a very thin 50 nm chromium adhesion layer. And Au is selected as the electrode material for its high electrical conductivity, good chemical, thermal stability, and suitability for wire bonding. To obtain a steady uniform thermal field in the central area, the heating electrodes are designed in a central symmetry structure with double helix shape with 12 µm width. A pair of interdigitated sensing electrodes, which fully contacts with the sensing layer, is located in the centre of heating electrodes with 15 µm width and 10 µm interval between the neighbouring interdigitated fingers. The sensing layer is defined as a square of $100 \times 100\ \mu m^2$, covered by the fingers of the sensing electrodes.

Fig. 3 shows the fabrication process, which can be divided into six main steps. Firstly, the SiO_2 layer with a thickness of 500 nm was grown by thermal oxidation on both sides of a 4 inches silicon wafer and then the Si_3N_4 layer with a thickness of 150 nm was deposited by low pressure chemical vapour deposition. After that, a 500 nm thick layer of SiO_2 and a 150 nm thick layer of Si_3N_4 were deposited on one side of the wafer by plasma enhanced chemical vapour deposition. To reduce the stress, the wafer was heated to 500°C for 6 h in air. Secondly, the pattern of sensing layer was defined by a photolithography process on the top side of the wafer. The TiO_2/SnO_2 nanocomposites were deposited by magnetron sputtering (Denton Vacuum, USA) using 3 inches TiO_2 and SnO_2 targets with purity of 99.99 and 99.99%,

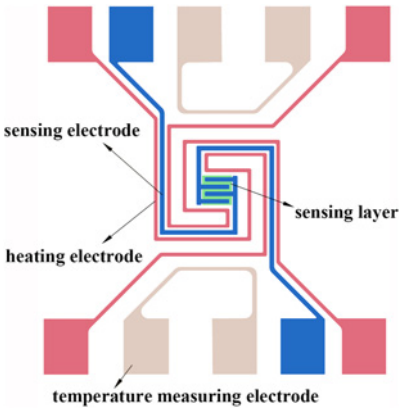

Fig. 2 *Top view of the microalcohol sensor chip*

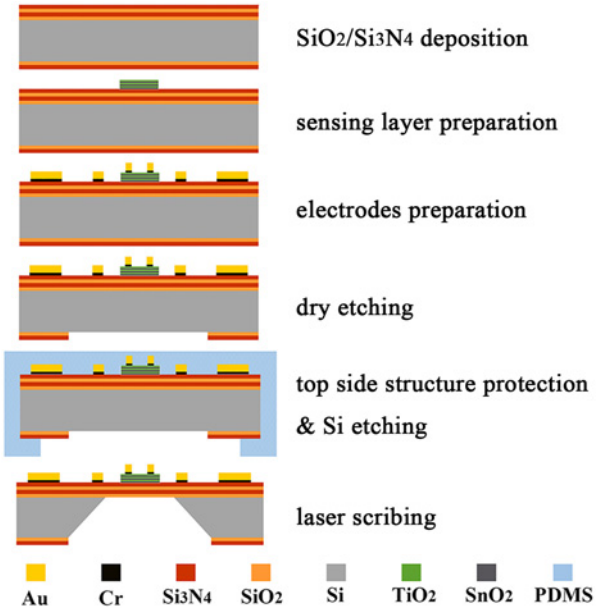

Fig. 3 *Fabrication process for integrated microalcohol sensor chips by using the MEMS process*

Table 1 Sputtering parameters for preparation of TiO_2/SnO_2 nanocomposites

Material	Power, W	Sputtering time, min
SnO_2	100	25
TiO_2	150	15
SnO_2	100	25
TiO_2	150	15
SnO_2	100	25
TiO_2	150	15

respectively. The sputtering parameters were listed in Table 1. Then, the sensing layer was patterned by a lift-off process and the wafer was annealed at 500°C for 3 h in air. Thirdly, the 50 nm thick of Cr and 250 nm thick of Au were patterned by a photolithography process and deposited by electron beam evaporation (HHY, TF500). Then the wafer was soaked in acetone for 12 h and a lift-off process was carried out. The wafer was heated to 300°C for 10 min to release the stress between the Cr/Au layer and substrate. Fourthly, the adiabatic groove on the back of silicon substrate was defined by the photolithography process. Then dry etching (Oxford, ICP-180) was used to remove part of Si_3N_4 and SiO_2 layers on the backside, which was not covered with the photoresist. The parameters of the dry etching are: the operating power is 800 W, CHF_3 is introduced into 70 sccm, and the time lasts for 13 min. In the fifth step, silicon exposed was released by wet etching using tetramethylammonium hydroxide (TMAH) solution with the concentration of 25%. Prior to that, the protection for the top side structure based on polydimethylsiloxane (PDMS) and glass was used to prevent sensing layer from corroding by alkali solution, more details about it can be found in our previous work [12]. The silicon can be removed completely in a TMAH solution at 85°C for 17 h. Finally, the 1.3 µm thick suspended membrane and adiabatic groove were remained. The wafer was sliced into individual chips by laser scribing.

3. Characterisation: The X-ray diffractometer (XRD, Panak) analysis of the TiO_2/SnO_2 nanocomposites was carried out for the Bragg angle (2θ) from 20° to 80°. The morphological

© The Institution of Engineering and Technology 2018

doi: 10.1049/mnl.2018.5183

characterisation and cross-section structure were observed by field emission scanning electron microscopy (FE-SEM, Zeiss, Gemini SEM 500). The elemental composition analysis and mapping of TiO_2/SnO_2 nanocomposites were carried out using an energy dispersive spectroscopy analysis (EDS, Oxford Instruments).

The sensing properties were measured using a computer controlled gas distributing system. The microsensor chip was attached to a testing circuit board using the heat-resistant adhesive and led to the pins by the gold wires with a diameter of 20 μm for testing. The sensor was placed in a small gas chamber, which has inlet and outlet for gases. To test its response to the alcohol gas, we blended the 1000 ppm alcohol gas and the synthesis air by two mass flow controllers (MFC, Seven Star CS200A) to provide different concentrations of alcohol gas. Total flow was kept at 200 sccm. Heating electrodes were connected in parallel with a DC power supplier to apply the voltage for heating, and the variation of sensing layer resistance between the sensing electrodes was monitored by a multimeter (Agilent 34410A) with a sampling frequency of 1 Hz.

4. Results and discussion: Fig. 4 depicts the XRD pattern of TiO_2/SnO_2 nanocomposite thin films consists of anatase phase of TiO_2 corresponding to (101), (200), (105), (211) and (204) planes at 25.281, 48.049, 53.890, 55.060 and 62.688 along with SnO_2 corresponding to (110), (101), (200), (211) and (112) planes at 26.611, 33.893, 37.949, 51.780 and 64.717.

Fig. 5 shows the morphology of the stacked TiO_2/SnO_2 nanocomposite films. The film surface has an irregular cluster consisting of the nanocrystal. Many cracks also appear on the surface, which can improve the gas adsorption ability by increasing specific area. The cross-section structure of the TiO_2/SnO_2 nanocomposite films can be seen from the top sight corner of Fig. 5. The layered structure of TiO_2/SnO_2 nanocomposite films can be clearly observed. The thickness of TiO_2 and SnO_2 thin films were found to be about 24.43 and 69.88 nm one layer, respectively.

As shown in Fig. 6, the yellow region of Ti, green region of Sn and the blue region of O are highly overlapped. The elemental mapping and EDS spectra of stacked TiO_2/SnO_2 nanocomposite films indicate the uniform element distribution of titanium, oxygen and stannum elements.

Fig. 7 shows the image of the microalcohol sensor chips after the MEMS fabrication process. Fig. 7*a* shows the image of the part fabricated integrated sensor chips array. There were 1700 sensor chips that can be fabricated in a 4 inches wafer, and about 85% sensor

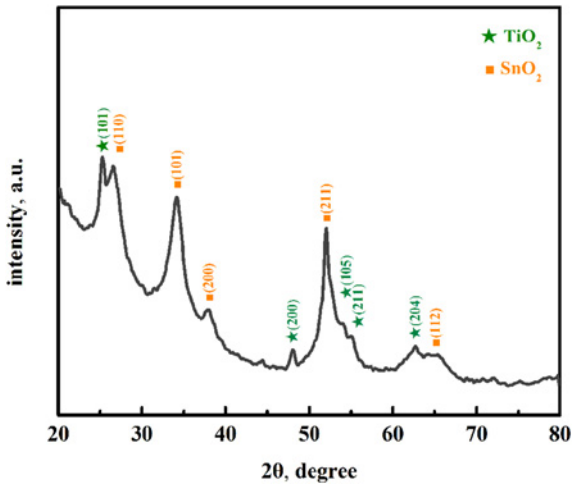

Fig. 4 *XRD pattern of the TiO_2/SnO_2 nanocomposite thin films*

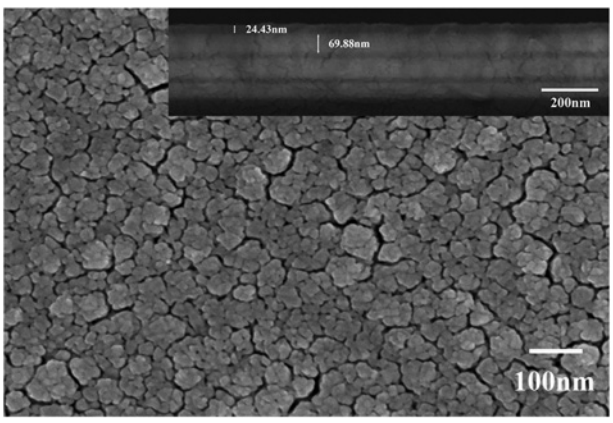

Fig. 5 *FE-SEM image and cross-section of TiO_2/SnO_2 nanocomposite thin films*

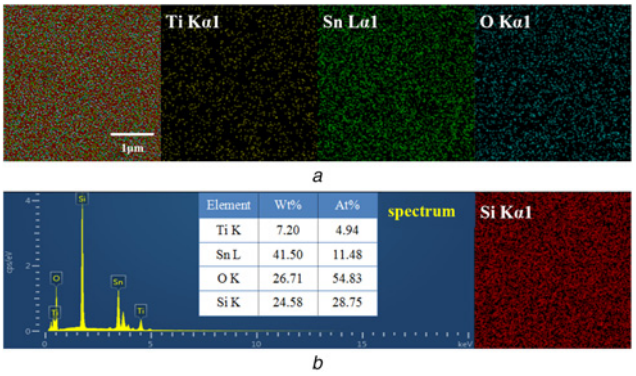

Fig. 6 *Elemental mapping and EDS spectra of TiO_2/SnO_2 nanocomposite thin films*
a Elemental mapping
b EDS spectra

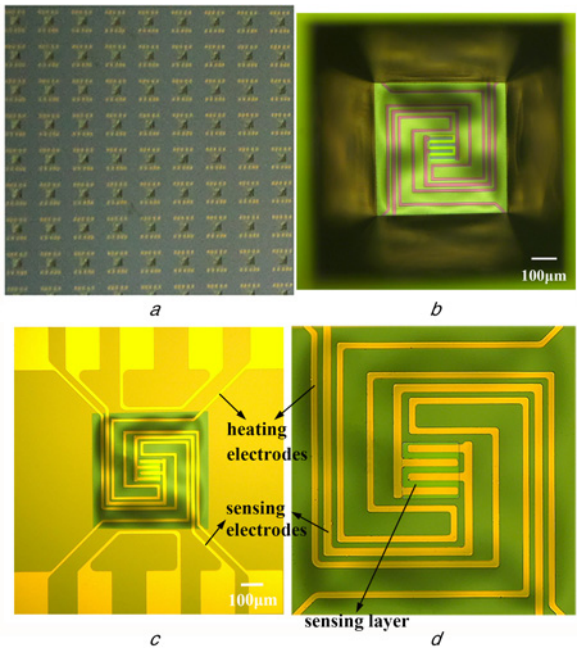

Fig. 7 *Image of the microalcohol sensor chips after the MEMS fabrication process*
a Fabricated integrated sensor chips array
b Sensor chip through the backside window after wet etching for the silicon substrate
c Structure from the top view of the fabricated integrated sensor chip
d Enlarged view of the central area

© The Institution of Engineering and Technology 2018

chips were intact observed by an optical microscope. So, the mass production of wafer-level microalcohol sensor chips can be realised through the designed fabrication process. According to the cost covering the fabrication process, the cost per sensor for 4″ wafer is estimated to be <80 cents in the high volume production. It is because we have adopted technologies such as magnetron sputtering which are compatible with MEMS technology that are more suitable for mass production. This is superior to the sensing film deposition method, such as the inkjet printing [14], sol–gel film deposition [15, 16]. The 1.3 μm thick suspended membrane of the adiabatic groove is transparent after the total release of Silicon, and the electrodes can be seen clearly from the back of the chip, as shown in Fig. 7*b*. Anisotropic corrosion of the (100) silicon wafer led to the trapezoidal groove, and the etched surfaces were smooth. In Figs. 7*c* and *d*, the up-down structures are well defined where electrodes exist on the transparent membrane with a sensing layer locating in the centre of interdigital electrodes as designed. The suspended membrane seems a little of crumpling on account of residual stress. However, it will not affect the normal work of the sensor, which can be verified by the subsequent experiments.

Three sensor chips were chosen from different regions of the wafer for response performance testing. The sensor response (S) is defined as the ratio of the initial resistance in synthetic air and resistance in target gas. Response time and recovery time were defined as the 90% time interval that the sensor took to equilibrate from one equilibrium state to another when the inlet gas concentration was changed

$$S = R_o/R_a \tag{1}$$

where R_o is the initial resistance in the synthetic air and R_a is the resistance in the presence of target gas.

The sensing layer resistance variation usually depends on the working temperature and target gas concentration exposed to the sensing materials. Firstly, to determine the optimum operating temperature, the gas sensing characteristics of microsensor chips were investigated at operating temperature of 148 − 320°C by measuring the change in resistance of the sensing electrodes upon exposure to 200 ppm alcohol gas, as shown in Fig. 8.

The results indicate that the sensor chips all exhibit a noticeable increase in response to rising the temperature up to 320°C. In view of the thermal annealing temperature of Cr/Au heating electrodes is 300°C and the sensor chip lifetime, the working temperature offered by microheater to sensing layer had not exceed 320°C better. So, the optimum working temperature is identified as 320°C with the highest response value of 18.57 towards 200 ppm alcohol gas. The power consumption is about 39 mW, which is much lower than the commercial semiconducting gas sensor and the previous works [5, 12]. Because of the double helix structure, the heat is more concentrated. Meanwhile, the design of back adiabatic groove also makes the heat loss not easy. These two points ensure the realisation of low power consumption.

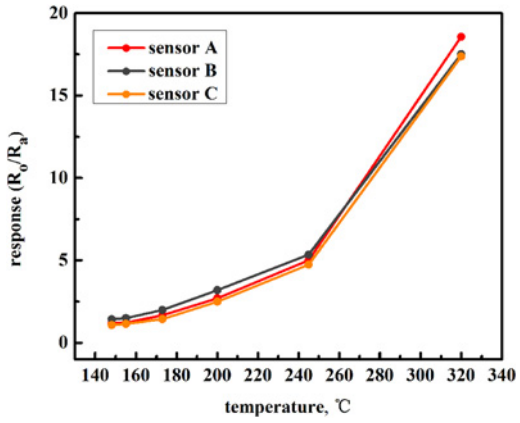

Fig. 8 *Response versus temperature in 200 ppm alcohol for alcohol sensor chips*

Fig. 9 shows the response of the microsensor chips exposed to different alcohol gas concentrations in the range of 50–600 ppm with power consumption of 39 mW. It is demonstrated that the different sensor chips have very similar responses at different alcohol gas concentrations. So, it is proved that the sensor chips possess good consistency. In general, sensor response increases with an increasing alcohol gas concentration. There results show that the sensor chip has the excellent response performance with response value of about 2.90–3.97 and 30.26–34.35 for 50 and 600 ppm alcohol gas, respectively. This may be attributed to the rough sensing layer surface consisting of the irregular cluster with the larger specific surface area and the formation of TiO_2/SnO_2 n–n heterojunction. The pure TiO_2 film is too dense, which leads to too little gas adsorption. It is the TiO_2/SnO_2 composite film that can solve the problem very well and improves the gas-sensitive response performance.

Fig. 10 shows the response curve of sensor chip A with 39 mW power consumption to different concentrations of alcohol gas. It is can be found that the response curve is very smooth without any fluctuation. This perhaps results from the stable concentrated heat reservoir offered by micro microheater, because any tiny temperature change will lead to the significant variation of the sensing material resistance.

The repeatability of the sensor chip is shown in Fig. 11, where the alcohol gas concentration was fixed at 50 ppm and the alcohol gas

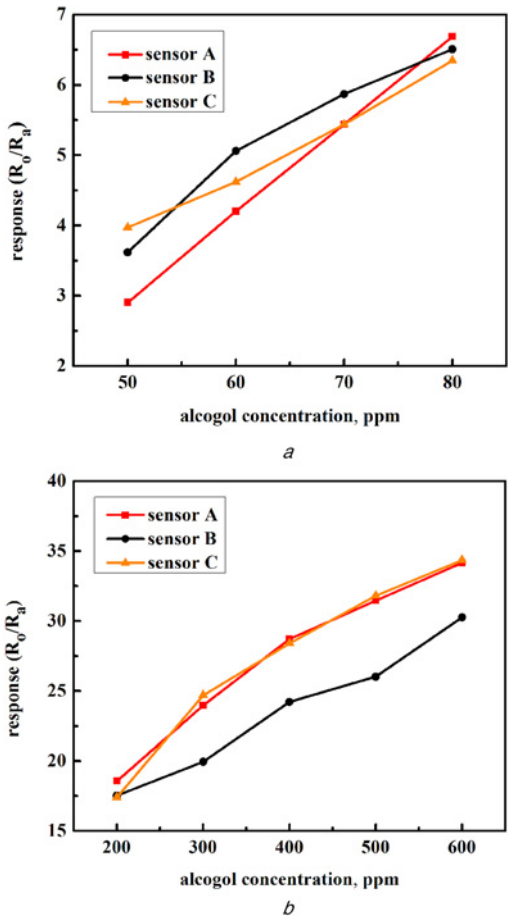

Fig. 9 *Response of sensor chips with 39 mW power consumption to different concentrations of alcohol gas*
a 50–80 ppm alcohol gas
b 200–600 ppm alcohol gas

© The Institution of Engineering and Technology 2018

doi: 10.1049/mnl.2018.5183

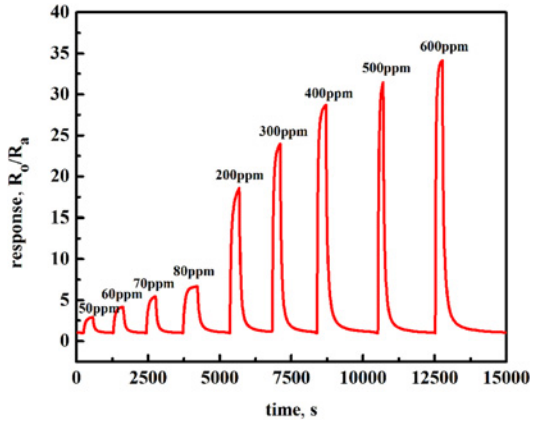

Fig. 10 *Response curve of sensor chip A with 39 mW power consumption to different concentrations of alcohol gas*

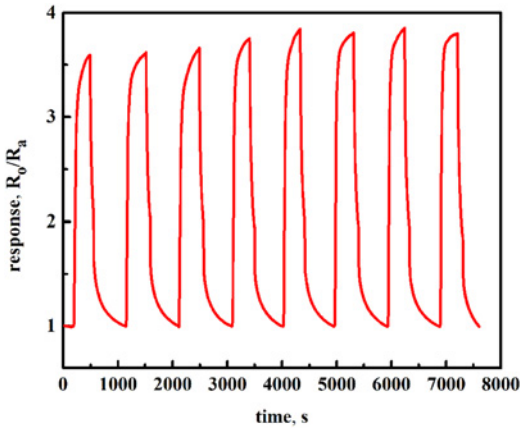

Fig. 11 *Repeatability of the microsensor chip for a constant alcohol gas concentration of 50 ppm*

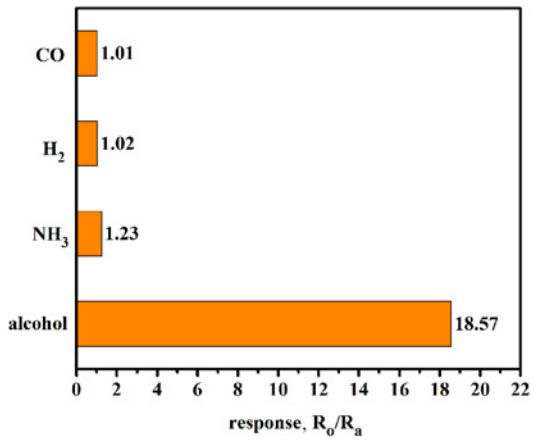

Fig. 12 *Responses of the sensor on exposure to other gases*

flow on and off time was about 5 and 10 min, respectively. The response curves are very similar to each other. It is indicated that the sensor chip has a good repeatability.

For the practical application of the sensors, the selectivity is a very important aspect. The selectivity experiment of sensor chip for alcohol, NH_3, H_2 and CO with the same concentration of 200 ppm at the optimum working temperature of 320°C has been conducted. The responses of the sensor to the above four gases were 18.57, 1.23, 1.02 and 1.01, respectively, as shown in Fig. 12. The excellent selectivity of the sensor chip was confirmed by the data of Fig. 12.

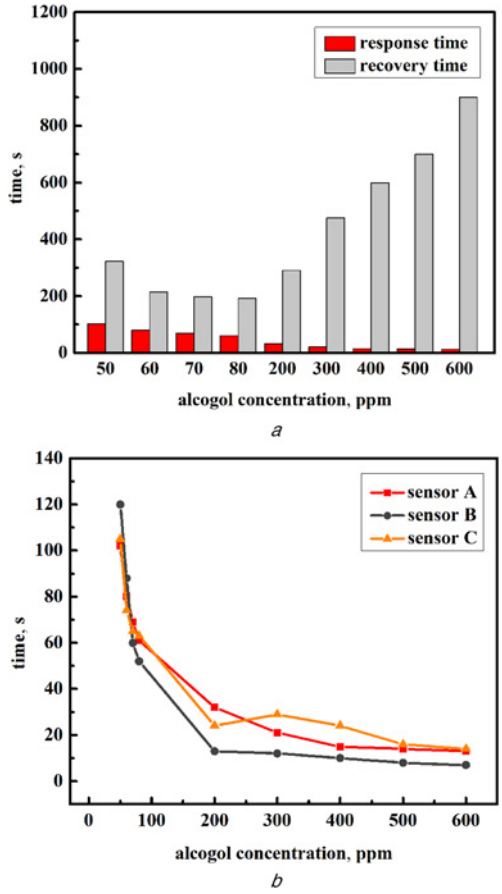

Fig. 13 *Response and recovery time of sensor chips with 39 mW power consumption*
a Response and recovery time of single sensor chip
b Curve of response time versus alcohol gas concentration of three sensor chips

Fig. 13*a* exhibits the response and recovery time characteristics of the single sensor chip to different alcohol gas concentrations, in which the response time significantly decreases and the recovery time has a tendency of getting longer with the alcohol gas concentration increasing. Response time and recovery time are about 102–14 and 193–900 s, respectively. The response times of the three sensor ships are compared, as shown in Fig. 13*b*. Their response times change in similar ways with the increasing alcohol gas concentration. The fastest response is accordingly confirmed, which is 7 s for 600 ppm alcohol gas. However, one should take in mind the sensor chips have a long recovery time. Hence efforts will be paid to solve this trouble in the future.

5. Conclusions: A microalcohol gas sensor based on TiO_2/SnO_2 nanocomposites was successfully developed by integrating the heating element and TiO_2/SnO_2 composite materials. The sensor was fabricated by MEMS technologies, characterised by various methods, and tested via the gas testing system. After the work we can draw the following conclusions:

A. An integrated microalcohol gas sensor, with an area of 2×2 mm^2, was designed. Sensing electrodes, sensing layers and heating electrodes were designed on the same layer to simplify the process. To reduce the power consumption, the silicon substrate under the central heating area with high thermal conduction was removed, thus a unique suspended membrane structure consisting

© The Institution of Engineering and Technology 2018

of $Si_3N_4/SiO_2/Si_3N_4/SiO_2$ four films fabricated by different methods, respectively, was remained to support above structures.

B. To solve the difficultly that the sensing layer preparation is incompatible with MEMS micromachining technologies, the process of six primary steps was determined to fabricate the gas sensor chips. The fabrication process can realise the mass production of the wafer-level sensor chips with good consistency. The yield can reach 85% and over 1400 sensor chips can be obtained on a 4 inches wafer.

C. The TiO_2/SnO_2 nanocomposites prepared by magnetron sputtering and annealing have higher sensitivity to alcohol gas. The microheater can provide a stable concentrated heat source in milliseconds. The microalcohol gas sensors show excellent response characteristics, including high sensitivity, good repeatability and fast response time for alcohol gas (50–600 ppm) at low power consumption (39 mW).

Owing to its small size, simple structure and excellent performance, the alcohol microgas sensors have good application potential. In the future study, our effort may turn to more MOS nanocomposites for reducing the detection limit and recovery time, as well as further lowering the power consumption of the sensor chip on a wafer level.

6. Acknowledgments: The work was supported by the National Nature Science Foundation of China (grant no. E51675420) and the National Key Research & Development (R&D) Program of China (grant no. 2016YFB0501604-02).

7 References

[1] Bănică F.G.: 'Chemical sensors and biosensors: fundamentals and applications' (Wiley, UK, 2012, 1st edn.)
[2] Shimizu Y.: 'Basic aspects and challenges of semiconductor gas sensors', *MRS Bull.*, 1999, **24**, (6), pp. 18–24
[3] Yamazoe N.: 'Toward innovations of gas sensor technology', *Sens. Actuators B, Chem.*, 2005, **108**, (1-2), pp. 2–14
[4] Barsan N., Koziej D., Weimar U.: 'Metal oxide-based gas sensor research: How to?', *Sens. Actuators B, Chem.*, 2007, **121**, (1), pp. 18–35
[5] Wang H., Wang J., Chen L., *ET AL.*: 'Integrated microoxygen sensor based on nanostructured TiO_2 thin films', *Micro Nano Lett.*, 2015, **10**, (10), pp. 597–602
[6] Simon I., Bârsan N., Bauer M., *ET AL.*: 'Micromachined metal oxide gas sensors: opportunities to improve sensor performance', *Sens. Actuators B, Chem.*, 2001, **73**, (1), pp. 1–26
[7] Sampson S.A., Date K.S., Panchal S.V., *ET AL.*: 'Investigation of QTF based gas sensors', *Sens. Actuators B, Chem.*, 2015, **216**, pp. 586–594
[8] Bhattacharyya P., Basu P.K., Mondal B., *ET AL.*: 'A low power MEMS gas sensor based on nanocrystalline ZnO thin films for sensing methane', *Microelectron. Reliab.*, 2008, **48**, (11), pp. 1772–1779
[9] Comini E., Baratto C., Concina I., *ET AL.*: 'Metal oxide nanoscience and nanotechnology for chemical sensors', *Sens. Actuators B, Chem.*, 2013, **179**, (2), pp. 3–20
[10] Benkstein K.D., Semancik S.: 'Mesoporous nanoparticle TiO_2 thin films for conductometric gas sensing on microheater platforms', *Sens. Actuators B, Chem.*, 2006, **113**, (1), pp. 445–453
[11] Zhou Q., Sussman A., Chang J., *ET AL.*: 'Fast response integrated MEMS microheaters for ultra-low power gas detection', *Sens. Actuators A, Phys.*, 2015, **223**, pp. 67–75
[12] Wang H., Yao Y., Sun Q., *ET AL.*: 'Design and fabrication of an integrated MEMS O_2 sensor based on nanostructured TiO_2', *Int. J. Nanotechnol.*, 2016, **13**, (10-12), pp. 764–777
[13] Wang H., Sun Q., Chen L., *ET AL.*: 'A micro room temperature O_2 sensor using the TiO_2 nanorod-based hierarchical nanostructures', *Ceram. Int.*, 2016, **42**, pp. 8565–8571
[14] Moon S.E., Lee H.K., Choi N.J., *ET AL.*: 'Low power consumption micro C_2H_5OH gas sensor based on micro-heater and ink jetting technique', *Sens. Actuators B, Chem.*, 2013, **187**, (4), pp. 598–603
[15] Li M., Yan W., Zhu H., *ET AL.*: 'Fabrication and characterization of a low power consumption ethanol gas sensor based on a suspended micro-hotplate', *RSC Adv.*, 2015, **5**, (64), pp. 1953–1960
[16] Fong C.F., Dai C.L., Wu C.C.: 'Fabrication and characterization of a micro methanol sensor using the CMOS-MEMS technique', *Sensors*, 2015, **15**, (10), pp. 27047–27059
[17] Dhivya P., Sridharan M.: 'Expeditious detection of ammonia using sputtered TiO_2 films', *J. Mater. Sci. Mater. Electron.*, 2015, **26**, (10), pp. 1–12
[18] Singh P., Kaur D.: 'Room temperature growth of nanocrystalline anatase TiO_2 thin films by dc magnetron sputtering', *Phys. B, Condens Matter*, 2010, **405**, (5), pp. 1258–1266
[19] Ryu S.W., Kim E.J., Ko S.K., *ET AL.*: 'Effect of calcination on the structural and optical properties of M/TiO_2 thin films by RF magnetron co-sputtering', *Mater. Lett.*, 2004, **58**, (5), pp. 582–587
[20] Liang Y.C., Lee C.M.: 'Cosputtering crystal growth of zinc oxide-based composite films: from the effects of doping to phase on photoactivity and gas sensing properties', *J. Appl. Phys.*, 2016, **120**, (13), p. 135306
[21] Kumar A., Sanger A., Kumar A., *ET AL.*: 'Fast response ammonia sensors based on TiO_2 and NiO nanostructured bilayer thin films', *RSC Adv.*, 2016, **6**, pp. 77636–77643
[22] Ponnusamy D., Prasad A.K., Madanagurusamy S.: 'CdO-TiO_2 nanocomposite thin films for resistive hydrogen sensing', *Microchim. Acta*, 2016, **183**, (1), pp. 1–7

© The Institution of Engineering and Technology 2018
doi: 10.1049/mnl.2018.5183